High-Precision OFDM-Based Multiple Ultrasonic Transducer Positioning Using a Robust Optimization Approach

Md. Omar Khyam, Md. Jahangir Alam, Andrew J. Lambert, Matthew A. Garratt, and Mark R. Pickering, *Member, IEEE*

***Abstract*— Ultrasonic positioning systems (UPSs) are used for various types of applications across a wide variety of fields, including robot navigation, device location, and pose estimation. In this paper, the focus is on investigating two major problems in the signaling and positioning the phases of existing UPSs and providing corresponding solutions. First, most of the existing UPSs use a single tone or a narrowband chirp signal for positioning, which suffer from multiple access due to signal interference. Second, if all reference points are placed in a single plane, which is logistically simpler for indoor applications and their distance from the target is larger than the distance between them, which is likely to happen, produced large dilution of precision errors when using lateration for position estimation. In this paper, first, to solve the multiple access problem, a narrowband orthogonal division-multiplexing signal, which can efficiently utilize the entire available frequency spectrum, is proposed. Second, a robust optimization approach for not only overcoming the limitation of the lateration algorithm but also ignoring errors in the distance measurements of the receivers corresponding to one complete cycle of the transmitted signal is proposed. The experimental results show that the proposed system has the precision required for high accuracy applications, and its cost and complexity are anticipated to be lower than those of alternative traditional optical systems.**

***Index Terms*— Multiple transducer positioning, sensor array, OFDM equalization.**

I. Introduction

THE location of a radiating source can be determined using information regarding its distances from at least three reference points, the locations of which are known [1]. This technique has been extensively used in research and production fields in many and varied applications, such as robot navigation [2]–[5], the precise location of instruments during laparoscopic surgery [6], and human movement tracking [7]–[25]. The general rationale for the system presented in this paper is the opportunity offered by ultrasound to conceive rather simple measurement methods or build comparatively cheap meters characterized by suitable accuracy, reduced measurement time and, above all, a high level of inherent safety [26].

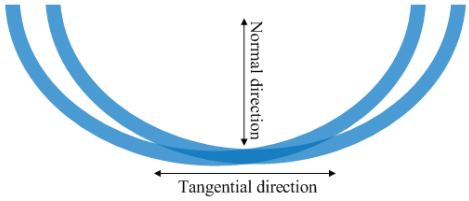

Fig. 1. Visualization of configuration related errors for the lateration algorithm when positioning targets.

In the past, several ultrasonic positioning and tracking systems have been developed which use either an active or passive mobile architecture. However, due to signal interference, all UPSs have difficulty simultaneously locating multiple *transducers*[1] in three-dimensional (3D) space when they use *narrowband*[2] transducers. Although they attempt to overcome this using time division multiplexing (TDM) techniques, that is, transmit the same pulse from collocated transmitters at different times, i.e., one after another with a proper interval to avoid signal interference at the receiving end. This leads to a slower update rate as only one transmitter is allowed to send at a time which limits the number of location updates possible in a given time interval [7], [27]. Therefore, this is not an efficient solution for applications for which simultaneous multiple transducers positioning is a prerequisite. Some methods for overcoming the multiple transducer access problem have been proposed using broadband transducers [14], [16], [28]–[33] that are more expensive than narrowband transducers.

A lateration algorithm is generally used in an UPS to obtain the target's location. For accurate (sub-millimeter) positioning of indoor reference points, it is simpler logistically if they are installed on a fixed plane. However, this configuration means that when lateration is used, the surfaces of the spheres centered at the reference points will be almost parallel when the separation between the reference points and target is larger than the separation between reference points which is likely to happen. This will produce larger errors in the positions of the intersecting points of the spheres for directions tangential

Manuscript received February 9, 2016; revised April 7, 2016; accepted April 11, 2016. Date of publication April 22, 2016; date of current version June 2, 2016. The associate editor coordinating the review of this paper and approving it for publication was Prof. Julian C. C. Chan.

M. O. Khyam is with the Faculty of Engineering, Department of Electrical and Computer Engineering, National University of Singapore, Singapore 117580 (e-mail: fahad_ete@yahoo.com).

M. J. Alam, A. J. Lambert, M. A. Garratt, and M. R. Pickering are with the School of Engineering and Information Technology, University of New South Wales at Canberra, Campbell, ACT 2612, Australia (e-mail: jahangir01326cse@yahoo.com; a.lambert@adfa.edu.au; m.garratt@adfa.edu.au; m.pickering@adfa.edu.au).

Digital Object Identifier 10.1109/JSEN.2016.2557817

[1]For an active mobile architecture the tracking or locating transducer(s) is the transmitter(s) and for a passive mobile architecture it is the receiver(s).

[2]If the the ratio of the bandwidth to the center frequency of a signal is less than 0.2, then the signal is considered to be narrowband.

to the surfaces of the spheres than for those normal to the surfaces, as shown in Fig. 1 with the shaded area due to the dilution of precision (DOP) effect. In addition, if the multipath issue is not solved properly at the measurement phase, errors can occur in the TOF of one complete cycle of the transmitted signal. However, lateration does not have the ability to eliminate such types of error from the position estimates.

In this paper, initially, to solve the multiple access problem, a narrowband OFDM signal, which can efficiently utilize the entire available frequency spectrum, is proposed. Then, a steepest descent optimization algorithm is proposed which overcomes the limitations of lateration approach and is also able to ignore errors in the distance measurements of receivers corresponding to one complete cycle of the transmitted signal.

The rest of this paper is organized as follows: Section II discusses related work, Section III details our proposed high-precision positioning system, a performance comparison between active and passive mobile architecture given in Section IV; Section V provides the experimental procedure for determining the precision of the proposed system, Section VI contains our experimental results and Section VII discusses the conclusions drawn from this study.

II. Related Work

A. Ultrasonic Spatial Locating System

An ultrasonic spatial locating system was proposed in [34] to locate points in three dimensions. Based on the transit time of a shock wave produced by a small electric spark, the position of one or more sparks was determined with respect to a coordinate system which was formed by 3 linear condenser (electret) microphones, arranged orthogonally, that detected the arrival of the wave front. The system incorporated a microcomputer-based processor and controller which was not only able to calculate the spatial coordinates from the measured transit times but also capable of self-calibration and error checking. An analysis of the system indicated that it was possible to locate points within a cube 50 cm on a side with an accuracy of less than 0.6 mm.

B. Kleeman's Autonomous Robot Location Systems

In an active mobile architecture, a two dimensional (2D) ultrasonic-based autonomous robot location system was presented in [35]. This system consists of a set of beacons placed at known position in a plane in the environment and an eight element ultrasonic receiver on board an autonomous robot. The beacons transmit 40 kHz ultrasonic chirps in fixed time sequence and the autonomous robot monitors the incoming chirps. From the fixed known time between beacon chirps and the speed of sound, which is calibrated from the initialization phase, arrival time differences of pulses are transformed in to the distance differences to the beacons. An iterative algorithm which uses the distance differences from three beacons provides solution of the robot's position and orientation in a plane by the intersection of hyperbolas. The robot position and orientation within a 10 meter square room was obtained to an accuracy of a few centimeters. The author extended the method from a 2D system to a 3D system in [36] where four beacons were utilized instead three to determine the 3D position of the robot. In [37], the same author presented two algorithms namely, the Geometrical Orientation Algorithm and the Iterated Extended Kalman filter approach to determine the position and orientation of the mobile robot. The first technique relies on a set of four direction measurements to geometrically evaluate the orientation of the receiver array. The second technique allows measurements to be smoothed in accordance with knowledge of motion statistics.

C. Active Bat

This was one of the first UPSs established by AT&T Research [38], [39] (1999) and, using an active mobile architecture, it consists of a group of mobile or fixed wireless transmitters (called bats) and ceiling-mounted receivers. Synchronization between the bats and receivers is achieved by sending RF pulses to them and, in response to the request of a RF pulse, a bat transmits an US pulse to the receivers which calculate their distances from the bat using the (velocity-difference) TDOA technique. From these measurements, the base station calculates the positions of the bats utilizing the multilateration algorithm. This system achieved a precision of 7 cm in a strongly controlled and centralized structural design.

D. Cricket

This is an US-based system which provides user-centric location support for ubiquitous applications and was developed at Massachusetts Institute of Technology in 2000 [40]. Using a passive mobile architecture, this indoor system consists of a set of beacons in the ceiling and receivers attached to the devices that require location. An RF signal is used to send the beacons' location information to the receivers and US pulses measure the distances between the receivers and nearby beacons which are used to find the positions of the receivers using the trilateration algorithm. This system has a reported precision of 10 cm and provides advantages in terms of scalability and privacy as it uses a passive mobile architecture but has the disadvantages that it lacks centralized management or monitoring and has a low coverage range due to the unidirectionality of its US transducers.

E. Low-Cost Indoor Positioning System

Using a passive mobile architecture Randell and Muller described a system [41] which allows wearable and mobile computers to autonomously compute their position. This system uses 4 US transducers, located at the corners of a square on the ceiling wired to a controller and a mobile device (MD) (receiver). The controller transmits a radio trigger followed by an US pulse from each of the 4 transmitters consecutively. The mobile receiver unit, synchronized by the radio trigger, calculates the TOF, from which it estimates its position with 3D accuracies between 10 and 25 cm.

F. Smith's System

To track a MD, a combination of active and passive mobile location architectures was proposed in [42] using

a Kalman filter (KF) and extended KF (EKF), with a method developed to transition between the passive and active modes of the MD. Until the KF's confidence is in a bad state, the MD (listener) does not transmit any information. It then becomes an active transmitter and generates simultaneous RF and US pulses, with the RF message having no information other than a randomly generated nonce which helps to hide the MD's identity. Whenever a beacon hears an RF message produced by a MD and its corresponding US pulse, it waits for a short random period of time and then broadcasts the nonce (set by the mobile) together with the distance estimate. After receiving this information from nearby beacons, the MD can accurately calculate its position, since the simultaneity condition holds for these distance samples, and then use this position estimate to reset its KF. The median error with passive, active and hybrid architectures at a speed of 1.43 m/s was reported as 22 cm, 4.7 cm and 14.9 cm respectively.

G. Huitema's System

This is an US motion analysis system which is capable of measuring temporal and spatial gait parameters while subjects walk on the floor [9]. It uses two US receivers, one attached to each shoe of the subject and a transmitter placed stationary on the floor. The transmitter transmits 8 consecutive pulses at intervals of 25 ms. The propagation delays for both receivers are measured using a bit counter that reaches its full range in 25 ms and begins counting the moment a burst is transmitted. When the transmitted burst is received by the US receivers, its output is stored and instantly converted to an analog output signal. Then, an input signal processor eliminates most noise from the input signal using a low-pass filter and testing of the minimum pulse strength. From their evaluation, at velocities of 0.85 m/s, 1.35 m/s and 1.91 m/s, the maximum toe-off errors were found to be 60 ms, 25 ms and 25 ms, and the heel-strike errors were 55 ms, 35 ms and 25 ms respectively.

H. BUZZ

This is an indoor positioning system presented in [43] which positions mobile computers using narrowband US signals, and involves the design and implementation of two novel systems, the synchronous and asynchronous BUZZ, each of which has a particular application. Positions are calculated through the use of transmission patterns, with the timing information communicated from the infrastructure to wearable receiving devices.

Synchronous BUZZ was an improvement proposed in [41] that eliminated the radio signal from the design which offers advantages in terms of clock synchronization, size and weight of the receiver. A central control unit connected to the beacons by wires is used to provide synchronization and, for positioning, an EKF and four beacon measurements are required. However, it has the limitation of the MD having to be placed in a particular location at start up. It calculates a 3D position with 4 cm precision 50% of the time and 10 cm precision 95% of the time, and its update rate is 33 Hz.

Asynchronous BUZZ is a wireless system like Cricket [40] but, as it does not use RF signals, it has advantages over Cricket in terms of system cost, power consumption and beacon sizes. Control of the transmission signal is decentralized and it is designed for low-precision applications. Its positioning error was within 50 cm.

I. Sato's System

This is an US motion capture system described in [18] and, using an active mobile architecture it consists of 5 US transmitters attached to the user's body and 4 US receivers acting as reference points. To avoid signal interference at the receiving end, each transmitter transmits a signal at a different time, i.e., it uses the TDM technique which reduces the system update rate. In the measurement phase, it uses a phase-based technique called the extended phase accordance method and, in the positioning phase, a multilateration algorithm. The accuracy achieved by this system was 4-5 cm.

J. Qi's System

This system measures 3D foot trajectories using a wearable wireless US sensor network in an active mobile architecture [24]. It consists of a narrowband US transmitter (mobile), 4 receivers (anchors) with known fixed positions and an RF module. To calculate the distance between the transmitter and receivers, it utilizes the (velocity-difference) TDOA technique. It applies pre-filtering in the range measurements to reduce the errors in tracking and localization, and then the pre-localization algorithm using the Newton-Gauss (NG) method filtered by an EKF. The experimental results showed that the proposed system had sufficient accuracy with a net root mean square error of 4.2 cm for 3D displacement, especially for foot clearance.

K. Hazas's System

This is the first broadband US location system proposed for achieving fine-grained location estimates [28], [29]. It provides advantages over narrowband systems in terms of signal interferences, data rates and noise sensitivity by using the direct sequence code division multiple access (DSCDMA) method. To generate the transmitted signal, a 50 kHz carrier wave is modulated by 51-bit-long Gold codes using binary phase shift keying (BPSK) and two types of positioning systems are proposed. The first is polled and centralized, which uses an active mobile architecture and has an accuracy of approximately 2 cm while the second is privacy-oriented, uses a passive mobile architecture and can be synchronous or asynchronous. The synchronous system utilizes the conventional multilateration algorithm along with cross-correlation to estimate the receiver's position whereas the asynchronous system uses direct-sequence pseudo-range measurements, and their system accuracies are 4.9 cm and 26.6 cm respectively.

L. Frequency Hopped Spread Spectrum (FHSS)

This positioning system was developed in [30] and uses broadband US signal. This system uses a set of fixed nodes at well-known locations called base stations (BSs) and MDs

whose positions and orientations are to be determined. The TOF and AOA are calculated by the MD using a circular array of transducers utilizing US and RF signals, with both direct sequence spread spectrum (DSSS) and FHSS signals used to provide a comparison of accuracy and robustness. The authors conclude that, using FHSS is more beneficial than DSSS, because only noise and multipath in the same band of frequencies affects the accuracy due to its variable carrier frequency. The experimental results show better accuracy for FHSS than DSS. FHSS provides a 3D estimation accuracy of less than 1.5 cm for 95% of cases

M. Reference-Free UPS

This system, which was developed in [31], utilizes broadband transducers and a FHSS technique. It does not require any reference signal for time synchronization between a transmitter and receiver and incorporates a new technique called the hybrid AOA-TOF which is an improvement over the conventional AOA technique. For TOF measurement, it uses the cross-correlation technique and its reported 3D precision is approximately 9.5 cm.

N. Code Division Multiple Access (CDMA)

This system is employed in an UPS in [32] for fine-grained location estimates. It uses four transmitters attached to the ceiling, with four distinct Gold codes generated and assigned to each of them. For location estimation, two methods are proposed. The first obtains the mean of four location estimates using the trilateration technique and, in the second, a single robust position estimate is obtained using only three distances while the least reliable fourth distance measurement is not considered. On the ground plane, the results show a 2 cm precision 99% of the time and 95% of the time when the MD is higher than the ground plane and near the ceiling respectively. However, all the experiments were conducted in a noise-free environment whereas, in a real indoor environment, the accuracy would be less and the hardware's complexity greater.

III. Proposed Method

A. Overview of OFDM

Basically, OFDM is a multicarrier system, in which the available frequency spectrum is divided into many narrowband channels, known as sub-carriers, which are dedicated to a single source. The main benefit of this approach being that multiple transmitters can transmit signals in parallel while maintaining high spectral efficiency.

Conceptually, OFDM is a type of FDM scheme which allows transmitters to transmit information across a communication channel in parallel and offers a more robust alternative to single carrier transmission systems in noisy communications channel that suffer from fading. OFDM offers much more efficient use of the available frequency spectrum than single tone and chirp signals.

The rapid increase in popularity for this scheme is due to the fact that it allows the available channel bandwidth to be used very efficiently. Due to its high spectral efficiency and resistance to multipath propagation, OFDM has been used for data transfer and positioning in wireless local area networks (WLANs) where data (bits) are modulated with RF sub-carriers and transmitted in parallel [44]–[53]. Due to the success of multicarrier modulation in the form of OFDM in radio channels it has drawn considerable attention for broadband ultrasonic (US) data transfer in both wired and wireless media [54]–[57]. Though the OFDM scheme has been used for US data transfer its performance still has not been investigated for UPSs.

By spacing the channels much closer together, OFDM uses the spectrum efficiently. This is achieved by making all the sub-carriers orthogonal to one another, avoiding interference between the closely spaced sub-carriers. These sub-carriers that do not interfere with each other are called orthogonal signals.

The spectrum of each sub-carrier may overlap with each other but remain orthogonal which means that the center frequency of each sub-carrier occurs at a null in the spectrum of all the other sub-carriers. Hence, OFDM transmission allows the carriers to be as close as theoretically possible. Since there is no signal interference between the sub-carriers this results in very high spectral efficiency. These orthogonal frequencies may be transmitted across a single communications channel. If signal orthogonality is maintained properly, at the receiving end they may be recovered without suffering from signal degradation resulting from interference from adjacent sub-carriers. In schemes such as TDM, temporal orthogonality is an inherent feature as only a single source out of a set of possible multiple sources is transmitted per timeslot. In non-OFDM systems such as FDM, the orthogonality is maintained by ensuring that the separate sources are spaced far enough apart in the frequency domain to ensure that no interference occurs. However, even though the sub-carriers are as densely packed as possible in OFDM, orthogonality is preserved by ensuring that all the sub-carrier baseband frequencies are integer multiples of the reciprocal of the signal period which is dependent on the sampling rate of the transmitter. This means that, all the sub-carriers have an integer number of cycles per period. In other words, in a particular time interval, each sub-carrier frequency is an integral multiple of a base frequency, and the number of cycles between two adjacent sub-carriers differs by exactly one.

Mathematically, two signals are said to be orthogonal if their dot product is zero which means that if they are multiplied and summed over an interval 0 to τ as described by equation (1), then the result is zero. Consider a set of signals $s_T(t)$. Orthogonality exists if:

$$\begin{aligned} \int_0^{\tau} s_{T_p}(t) s_{T_q}^*(t) dt &= k \quad \text{for } p = q \\ &= 0 \quad \text{for } p \neq q \end{aligned} \tag{1}$$

where $s_{T_p}(t)s$ and $s_{T_q}(t)$ are the p-th and q-th elements in the set, * denotes the complex conjugate of the signal and $[0, \tau]$ is the signal length. To make the sub-carriers orthogonal the separation between sub-carriers must be $(1/\tau)$. The sub-carrier's orthogonality can be observed in either the

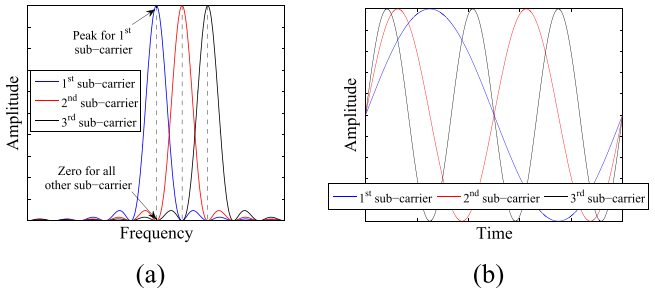

Fig. 2. Visulization of three orthogonal sub-carriers of an OFDM signal in: (a) frequency domain and (b) time domain.

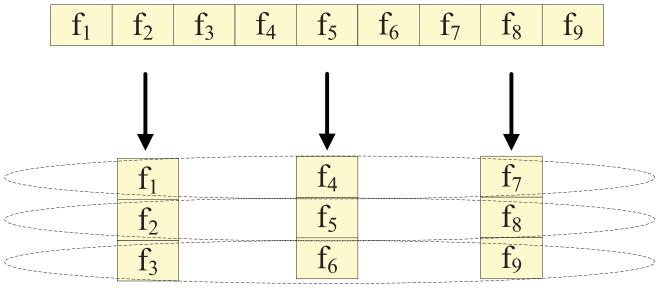

Fig. 3. Frequency allocation in an OFDM system for positioning in active and passive mobile architectures.

time domain or in the frequency domain. From the frequency domain perspective, the center frequency of each sub-carrier occurs at a null in the spectrum of all the other sub-carriers i.e., orthogonality in an OFDM system occurs when at the peak of each sub-carrier spectrum, the contribution from all other sub-carries is zero as shown in Fig. 2(a). From the time domain perspective, each sub-carrier is a sinusoid with an integer number of cycles within the signal period and the number of cycles between two adjacent sub-carriers differs exactly by one as shown in Fig. 2(b).

From the above discussion the main major advantage of using an OFDM signal in the field of UPS is OFDM offers much more efficient use of the available spectrum than single tone and chirp based positioning system due to the simultaneous use of multiple frequencies for data transmission.

Each sub-carrier of an OFDM signal is represented by $A_T(t)e^{j2\pi ft}$ where f and $A_T(t)$ represent the frequency and amplitude of the sub-carrier respectively. Generally, an OFDM waveform is created in the frequency domain initially and then converted to a real-valued time domain waveform using the inverse fast Fourier transform (IFFT). In order to correctly create the time domain waveforms, the conjugate of the real sub-carrier values (the imaginary frequency components) must be inserted into the fast Fourier transform (FFT) array. The following section presents pictorial and mathematical representations of the OFDM technique for simultaneous multiple transducer positioning.

1) OFDM Signal for Multiple Transducer Positioning: The OFDM based multiple transducer positioning system works in a three stage process. In the first stage, all the available orthogonal frequency components are placed serially as shown in Fig. 3 where there are nine orthogonal frequency components ($f_1, f_2, \cdots, f_9$). Although only nine sub-carriers are illustrated, the number of sub-carriers may be higher depending on the bandwidth.

The second stage involves converting all the frequency components into a number of shorter parallel sub-sets. In active and passive mobile architectures, the number of sub-sets is equal to the number of transducers to be localized and the number of transducers to be used as reference points respectively. For example, continuing on from the example shown in Fig. 3, suppose it is required to localize three transducers in an active mobile architecture or three transducers are to be used as reference points in a passive mobile architecture. This means that the number of sub-sets will be three in both cases where each of which contains three frequency components (shown in the Fig. 3).

In the final stage, using all the frequency components contained in each sub-sets, an OFDM signal is generated for each transmitter (indicated by the dash circle in Fig. 3). Though all the OFDM signals are transmitted in parallel from the individual transmitter, the receivers received these signals without any interference as they use different bands i.e., non-overlapping frequency components.

The number of sub-sets is equal to the number of transducers to be localized in an active mobile architecture and number of transducers to be used as reference points in a passive mobile architecture. Therefore, a passive mobile architecture offers better scalability because, when using only three reference points (minimum), it would be able to calculate any desired number of transducers within the operating environment as the wireless channel is not dependent on the number of devices which to be localized.

This phenomenon can also be described mathematically as described below.

2) Mathematical Model of OFDM Signals for Multiple Transducer Positioning: If the sampling frequency of a signal is F_s and its length is N samples, the frequency resolution is $r_s = \frac{F_s}{N}$. Letting the lower carrier of the desired OFDM signal be f_l and the upper carrier f_u, i.e., a bandwidth of $W = f_u - f_l$. As the frequency resolution is r_s, the available orthogonal frequency components are:

$$f = \{f_l, f_l + r_s, f_l + 2r_s, \cdots, f_u\} \tag{2}$$

Now, if a represents the number of transmitters, A and θ indicate the amplitude and phase of each carrier respectively, and n represents the number of sample points in the frequency domain, the frequency domain OFDM signal distributed to the transmitters is given by:

$$X_{a,i,c}[n_{a,i,c}] = \begin{cases} A[n_{a,i,c}]e^{j\theta[n_{a,i,c}]} & \text{where } n_{a,i,c} = \frac{f_l}{r_s} + \frac{\Delta f(i-1)}{ar_s} + \frac{\Delta f(c-1)}{r_s} \\ A[n_{a,i,c}]e^{-j\theta[n_{a,i,c}]} & \text{where } n_{a,i,c} = N + 1 \times \left(\frac{f_l}{r_s} + \frac{\Delta f(i-1)}{ar_s} + \frac{\Delta f(c-1)}{r_s}\right) \\ 0 & \text{elsewhere} \end{cases} \tag{3}$$

Algorithm 1 Pseudo Code of the Narrowband OFDM Signals for Multiple Transducers Positioning

```
• Set, f_l, f_u, N
• Calculate r_s
• Calculate Δf
• for a = 1 : f_u/r_s do
    for i = 1 : a do
        for c = 1 : W/Δf do
        Calculate n_{a,i,c}
        end for
    end for
end for
```

where Δf is the frequency gap between two sub-carriers in each OFDM signal (which depends on the number of transmitters to be used in the system) and c is the number of frequency components present in each OFDM signal. The value of Δf is given by:

$$\Delta f = ar_s \tag{4}$$

For each a, i is given as:

$$i = 1, 2, \cdots, a \tag{5}$$

and the value of c is given as:

$$c = 1, 2, \cdots, \frac{W}{\Delta f} \tag{6}$$

For the active mobile case, equation (4) states that, for a fixed frequency resolution, the more transmitters to be localized, the greater the frequency separation (Δf) between adjacent sub-carriers. However, according to equation (6), there are fewer frequency components which means that when the OFDM signal becomes a single tone signal. Therefore, the accuracy of the cross-correlation based TOF estimation technique will be low. On the contrary, a passive mobile architecture would be able to localize any desired number of transducers within the operating environment as the wireless channel is not dependent on the number of transducers to be localized in this approach.

In summary, the signal design process for multiple transducers positioning can be explained through the pseudo-code:

B. Equalization

In our proposed method, five known OFDM signals each composed of fixed orthogonal signals containing the frequency components $f_c (c = 1, 2, \ldots, n)$, which range from 35 kHz to 45 kHz with a fixed frequency gap is transmitted according to the procedure described in Section III-A2. The sampling frequency (F_s) was 1 MHz and the length (N) of each signal was 10000 samples (in the frequency domain). As all the components have equal amplitudes and phases, the resultant OFDM signal is a narrowband approximation of an impulse and the FFTs of the transmitted and received signals are given by:

$$S_T = \Im(t) = m_t e^{j\theta_{s_t}} \tag{7}$$

$$S_R = \Im(r) = m_r e^{j\theta_{s_r}} \tag{8}$$

where $\Im$ denotes the FFT operation and m and θ the magnitude and phase components of each signal respectively.

Firstly, an equalization technique is required to achieve an overall linear phase response of the US transducer. The frequency response of transducers can be modelled by placing the transmitter and a receiver face to face so that the length of the wireless channel between the transmitted and received signals is effectively zero. Now the inverse frequency response of the transducers G which is called an equalizer or frequency response compensator is given by:

$$G = \left(\frac{S_T(f_c)}{S_{R_p}(f_c)}\right) \tag{9}$$

where S_T and S_{R_p} represent the transmitted and received signals in the frequency domain respectively and f_c the specific transmitted frequency components. To eliminate the effect of the transducers and reduce noise significantly from the received signals, each received signal in the frequency domain (S_R) is multiplied by G and the IFFT calculated. Mathematically, the equalized received signal ($s_{R_{eq}}$) is defined as:

$$s_{R_{eq}} = \Im^{-1}(S_{R_{th}} G) \tag{10}$$

The ToF between the transmitter and each receiver is then estimated by locating the position of the received OFDM signal in time using cross-correlation with the transmitted signal.

C. Transducer Localization Using Steepest Descent Optimization

For this step in the process, five reference points are considered and the ideal positions of their centers (in cm) are given in the following matrix.

$$\mathbf{P} = \begin{bmatrix} -30 & -30 & 0 \\ 0 & 0 & 0 \\ 30 & -30 & 0 \\ -30 & 30 & 0 \\ 30 & 30 & 0 \end{bmatrix}$$

The reference points are mounted in a single plane (at $z = 0$ in the proposed coordinate system) and their positions relative to the transducers which are to be localized are illustrated in Fig. 4. In practice, these ideal positions are slightly modified after calibration to account for any inaccuracies in the mounting process.

The purpose of the proposed optimization approach is to determine the relative positions of the reference points and target transducer which best correspond to the distances measured by the TOF of the US signal. To fulfil this objective, it is initially assumed that the transducer which is to be localized is placed at the same position as reference point R_2, i.e., (0, 0, 0). Then, to estimate the positions of the reference points with respect to the transducer, a steepest descent optimization approach is used to determine the translation in the z direction and rotations around the x and y axes of the reference plane which places the five reference points at positions which best correspond to their measured distances

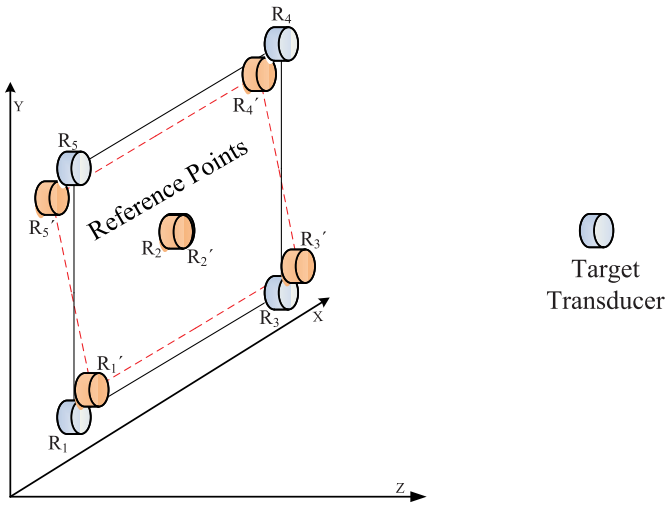

Fig. 4. Deviation of receiver plane.

from the transducer. Fig. 4 illustrates the positions of the reference points (in yellow) after the reference plane's rotation around its x axis. This optimization problem corresponds to finding the matrix ($\mathbf{M}$) which minimizes the error:

$$E = \sum_{r=1}^{5} (\| \mathbf{M}\mathbf{p}_r^{(0)} \| - d_r)^2 \tag{11}$$

where $\mathbf{p}_r^{(0)} = [x_r^{(0)} \quad y_r^{(0)} \quad z_r^{(0)} 1]^T$ is the initial position of reference point r in homogeneous coordinates, d_r is the distance from the transducer (which to be localized) to reference point r estimated from the TOF and $\mathbf{M}$ a specific three-dimensional (3D) rigid-body transformation consisting of rotations around the x and y axes (R_x and R_y respectively) followed by a translation in the z direction (T_z).

These parameters define the transformation matrix $\mathbf{M}$ as:

$$\mathbf{M} = \mathbf{T}\mathbf{R} \tag{12}$$

where $\mathbf{T}$ is the translation matrix given by:

$$\mathbf{T} = \begin{bmatrix} 1 & 0 & 0 & 0 \\ 0 & 1 & 0 & 0 \\ 0 & 0 & 1 & T_z \\ 0 & 0 & 0 & 1 \end{bmatrix}$$

and the rotation matrix around the x and y axes ($\mathbf{R}$) is given by:

$$\mathbf{R} = \begin{bmatrix} \cos(R_y) & 0 & -\sin(R_y) & 0 \\ -\sin(R_x)\sin(R_y) & \cos(R_x) & -\sin(R_x)\cos(R_y) & 0 \\ \cos(R_x)\sin(R_y) & \sin(R_x) & \cos(R_x)\cos(R_y) & 0 \\ 0 & 0 & 0 & 1 \end{bmatrix}$$

Then, the steepest descent optimization approach is required to find the optimum values of T_z, R_x and R_y.

For iteration n of the optimization, the new positions of the reference points are given by:

$$\mathbf{p}_r^{(n)} = [x_r^{(n)} \quad y_r^{(n)} \quad z_r^{(n)} \quad 1]^T = \mathbf{M}^{(n)}\mathbf{p}_r^{(0)} \tag{13}$$

where the values of the transformation parameters are given by:

$$\mathbf{m}^{(n+1)} = \mathbf{m}^{(n)} - \alpha \nabla \mathbf{E} \tag{14}$$

where α is a constant step size,

$$\mathbf{m} = [T_z \quad R_x \quad R_y]^T \tag{15}$$

and

$$\nabla \mathbf{E} = \left[\frac{\partial E}{\partial T_z} \quad \frac{\partial E}{\partial R_x} \quad \frac{\partial E}{\partial R_y}\right]^T \tag{16}$$

The elements of $\nabla \mathbf{E}$ are defined as:

$$\frac{\partial E}{\partial T_z} = 2\sum_{r=1}^{5} \frac{(\|\mathbf{p}_r^{(n)}\| - d_r)}{\|\mathbf{p}_r^{(n)}\|}(T_z^{(n)} + \cos(R_x^{(n)})\sin(R_y^{(n)})x_r^{(0)} + \sin(R_x^{(n)})y_r^{(0)} + \cos(R_x^{(n)})\cos(R_y^{(n)})z_r^{(0)}) \tag{17}$$

$$\frac{\partial E}{\partial R_x} = 2\sum_{r=1}^{5} \frac{(\|\mathbf{p}_r^{(n)}\| - d_r)}{\|\mathbf{p}_r^{(n)}\|}(-\sin(R_x^{(n)})\sin(R_y^{(n)})T_z^{(n)}x_r^{(0)} + \cos(R_x^{(n)})T_z^{(n)}y_r^{(0)} - \cos(R_y^{(n)})\sin(R_x^{(n)})T_z^{(n)}z_r^{(0)}) \tag{18}$$

$$\frac{\partial E}{\partial R_y} = 2\sum_{r=1}^{5} \frac{(\|\mathbf{p}_r^{(n)}\| - d_r)}{\|\mathbf{p}_r^{(n)}\|}(\cos(R_x^{(n)})\cos(R_y^{(n)})T_z^{(n)}x_r^{(0)} - \cos(R_x^{(n)})\sin(R_y^{(n)})T_z^{(n)}z_r^{(0)}) \tag{19}$$

If $e_r = 2(\|\mathbf{p}_r^{(n)}\| - d_r)$ and it is assumed that R_x and R_y are small, these expressions can be simplified to give:

$$\frac{\partial E}{\partial T_z} \approx \sum_{r=1}^{5} \frac{1}{\|\mathbf{p}_r^{(n)}\|} e_r z_r^{(n)} \tag{20}$$

$$\frac{\partial E}{\partial R_x} \approx \sum_{r=1}^{5} \frac{T_z^{(n)}}{\|\mathbf{p}_r^{(n)}\|} e_r y_r^{(0)} \tag{21}$$

$$\frac{\partial E}{\partial R_y} \approx \sum_{r=1}^{5} \frac{T_z^{(n)}}{\|\mathbf{p}_r^{(n)}\|} e_r x_r^{(0)} \tag{22}$$

Then, to minimize the effect of the outliers in the e_r terms, that are proportional to one complete cycle of the transmitted signal, the summation is replaced by a median operation. The median estimator is a robust statistic [58] and is therefore better able to estimate the true arrival time when outliers in the data are present. Since the summation is replaced by the median operator, the step-size (α) is divided by the number of receivers. One disadvantage of this approach is that the convergence speed will increase slightly since the median operation involves a data sorting procedure. This steepest descent optimization approach is guaranteed to converge to a global minimum because the error function, given in equation (11), is convex [59].

Once the optimization converges to a solution (usually within 10 iterations), the position of the transducer is calculated with respect to the initial position of the reference plane using the inverse of the optimum value of $\mathbf{M}$:

$$\mathbf{p}_t = \mathbf{M}^{-1}\begin{bmatrix} 0 & 0 & 0 & 1 \end{bmatrix}^T \tag{23}$$

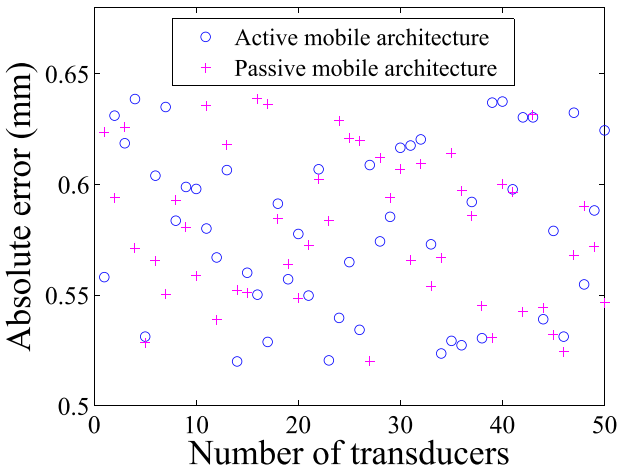

Fig. 5. Absolute location errors of the proposed method in both active and passive mobile architectures.

Using this approach, the transducer's positions can be calculated.

In summary, the proposed steepest descent positioning algorithm is implemented as follows and requires iterations of steps 1 to 3 until the optimization converges to a solution.

- **Step 1:** initialize 1) the reference point's coordinates ($\mathbf{p}_r^{(0)}$), 2) the distance (d_r) from the transducer (which to be localized) to reference point r estimated using the proposed TOF technique and 3) the translation in the z direction (T_z), and rotations around the x and y axes (R_x and R_y respectively).
- **Step 2:** calculate the 3D rigid-body transformation matrix ($\mathbf{M}$) using equation (12) and the error (E) using equation (11).
- **Step 3:** if E from step 2 has not converged to a solution, update the transformation parameters (T_z, R_x, R_y) using equation (14) and then go back to step 2; else calculate the transducer's position using equation (23).

IV. Simulation Results

A customized environment was simulated in Matlab to evaluate the performance of the proposed UPS. In this simulator, in a virtual 3D rectangular room, five reference points were considered and 50 transducers were introduced with the aim of localizing these using both passive and active mobile architectures. The true positions of the target transducers were known. The location of the five reference points were as follows:

$$\mathbf{P} = \begin{bmatrix} -30 & -30 & 0 \\ 0 & 0 & 0 \\ 30 & -30 & 0 \\ -30 & 30 & 0 \\ 30 & 30 & 0 \end{bmatrix}$$

The simulation was performed in a noisy multipath environment (5 paths at random positions) with reflection coefficients of 0.9 to 0.5, and the corresponding attenuation of the signal was calculated using the formula $A = A_0\, e^{-\gamma d}$, where A_0 is the unattenuated amplitude of the propagating wave at a location, A the reduced amplitude after the wave has traveled a distance (d) from that initial location and γ the attenuation coefficient of the traveling wave in the d direction. In both active and passive cases, [35–35] kHz/10 ms OFDM signals (i.e., the length of the signal is 10 ms and, its initial and final frequencies are 35 kHz and 45 kHz respectively) were used where frequency components were allocated to the reference points in the passive mobile architecture and to the transducers to be localized in the active mobile architecture according to the procedure described in Section III-A2. The position of the target transducers were calculated in both mobile architectures using the steepest decent optimization algorithm described in Section III-C using the TOF information calculated using the procedure described in Section III-B. The absolute location errors (calculated using the Euclidean distance between true and estimated positions) of the target transducers in both architectures is shown in Fig. 5 which shows that the accuracy, in a multipath environment, for both architectures is almost the same. But it is important to note that, in an active mobile architecture it was not possible to localize more than 50 transducers as frequency components were limited whereas in a passive mobile architecture it was possible to localize any desired number of transducers within the operating environment as the wireless channel did not depend on the target transducers.

This section describes how a narrowband-based UPS can utilize the whole effective bandwidth for multiple transducer positioning. The method is also valid for broadband UPSs.

V. Experimental Procedure

To evaluate the proposed OFDM-based multiple transducer positioning system described in Section III-A2, two separate experiments were conducted (in indoor noisy and multipath environments) for both active and passive mobile architectures where the number of transducers to be localized and number of reference points was five. Piezotite MA40S4S and MA40S4R ultrasonic devices were used as transmitters and receivers which can effectively utilize 10 kHz of the frequencies centered around 40 kHz. The configuration of the experimental setup was as shown in Fig. 4, except the number of transducers to be localized were five instead one. The configuration of the reference points is shown in Fig. 6(a). Although 9 receivers are visible in Fig. 6(a), only the central and corner receivers were used. The target transducers were separated by a fixed offset and moved to 20 different locations inside a 20×20×20 mm volume, and the true positions were measured using a Vernier scale (shown in Fig. 6(b)) with a precision of 0.02 mm. The boundaries of the transducers movements were restricted to 20 × 20 × 20 mm because the range of the Vernier scale used for the experiments was limited to this volume. However, the transducers can be moved anywhere within the operating environment. In both cases, [35–45] kHz/10 ms OFDM signals were used where frequency components were allocated to the reference points in a passive mobile architecture and to the transducers which to be localized in an active mobile architecture according to the procedure described in Section III-A2.

(a) (b)

Fig. 6. Experimental setup: (a) configuration of the reference plane and (b) Vernier scale.

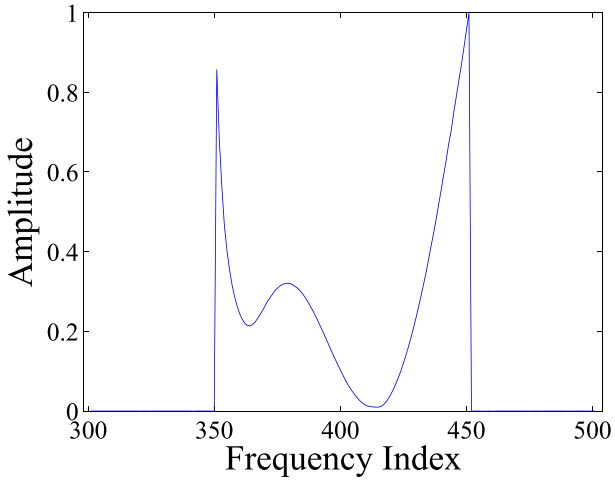

Fig. 7. Inverse frequency response of the transducer.

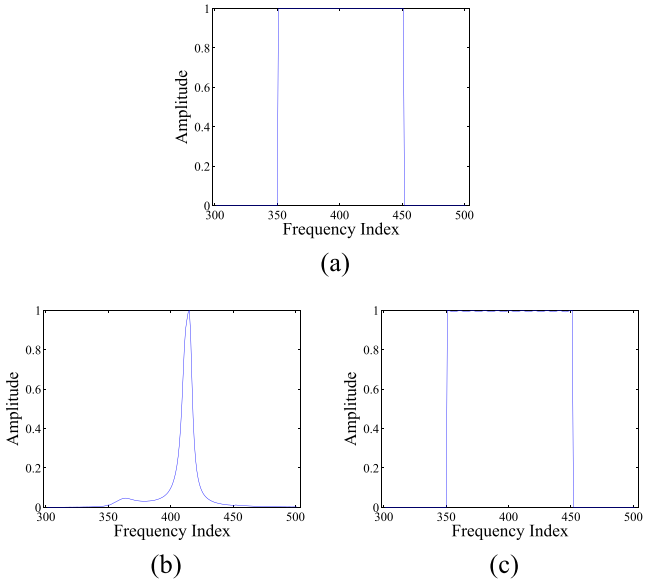

Fig. 8. Frequency response of the: (a) transmitted signal; (b) received signal; and (c) equalized received signal.

To demonstrate the improvement in accuracy provided by the proposed approach, the positions of the target transducers were also calculated by the traditional cross-correlation-based multilateration algorithm for both architectures using [35–45] kHz/10 ms chirp signal through TDM technique i.e., chirp signals were transmitted at different times from the transmitters to avoid the signal interference which reduces the positioning update rate.

VI. Results and Analysis

Before performing the experiments in both active and passive mobile architectures for multiple transducer positioning, the inverse frequency response of the transducers G (using equation 9) was calculated by placing the transmitter and a receiver face to face so that the length of the wireless channel between the transmitted and received signals is effectively zero. The response obtained from that is shown in Fig. 7. To visualize the proposed TOF technique described in Section III-B, a test case (from the experiments described in the earlier section) was analysed. In this case, Fig. 8(a) shows the frequency response of the transmitted OFDM signal a frequency range of 35 kHz to 45 kHz. The shape of the received OFDM signal shown in Fig. 8(b) was not the same as that of the transmitted signal because of the transducer, noise and multipath effects. Fig. 8(c) shows the frequency response of the equalized received signal (using equation 10) which had an almost similar frequency response to the transmitted signal. Hence the equalization technique improved the accuracy of TOF estimation by removing the transducer response and reducing noise and multipath effects.

After completing the experiments in both active and passive mobile architectures for multiple transducer positioning (described in earlier section), the position of each transducer was calculated for the both proposed and traditional methods. The combined errors of the x, y and z directions in the calculated locations of all transducers using the proposed and traditional approaches in both architectures are shown in Fig. 9 and Fig. 10 respectively and the standard deviations of these errors in each direction are shown in Table I.

TABLE I

STANDARD DEVIATIONS OF ERRORS IN THE MEASURED LOCATIONS OF THE TRANSDUCERS IN BOTH ACTIVE AND PASSIVE MOBILE ARCHITECTURES (mm)

Number of Transducer	Architecture											
	Active						Passive					
	Proposed			Traditional			Proposed			Traditional		
	x	y	z	x	y	z	x	y	z	x	y	z
1	0.3117	0.3240	0.3145	9.8011	9.7268	1.5510	0.3245	0.3195	0.3176	9.8011	9.7268	1.5510
2	0.3420	0.3085	0.3042	9.7159	9.6940	1.5894	0.3183	0.3164	0.3206	9.7159	9.6940	1.5894
3	0.3260	0.3045	0.3293	9.6434	9.9123	1.5851	0.3142	0.3156	0.3276	9.6434	9.9123	1.5851
4	0.3350	0.3325	0.3321	9.3386	9.9555	1.5323	0.3203	0.3141	0.3245	9.3386	9.9555	1.5323
5	0.3261	0.3329	0.3084	9.8633	9.9687	1.5429	0.3165	0.3273	0.3240	9.8633	9.9687	1.5429

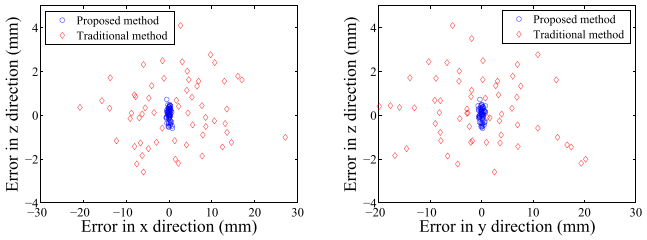

Fig. 9. Errors in location of the transducers from the proposed and trilateration methods in an active mobile architecture.

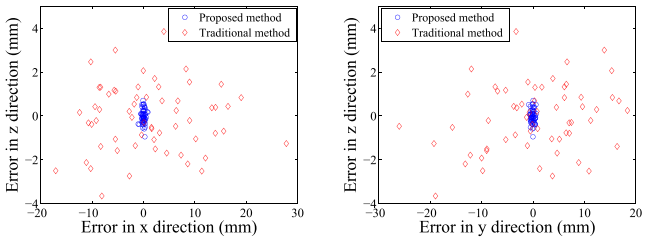

Fig. 10. Errors in location of the transducers from the proposed and trilateration methods in a passive mobile architecture.

These results show that the precision obtained using the proposed method, in a multipath environment, was significantly higher and provided the sub-millimeter accuracy required for many high accuracy applications. It should be noted that the calculated location errors for the traditional TDM-based technique for both active and passive mobile architectures are almost the same. This is because the targets were static and thus there was no impact on the system performance by the motion of the targets. However, for the positioning of moving targets, the system performance for both architectures will be different [42]. The proposed method did not suffer from the lower positioning update rate like the TDM-based traditional method. It is also important to note that, the scalability of the passive mobile architecture was not bounded by the frequency components like the active mobile architecture.

VII. CONCLUSIONS

In this paper, initially it was proposed to use OFDM signals to achieve simultaneous multiple transducer positioning which offers the unique features of: efficiently utilizing the bandwidth; no affect on the update rate; and reduced system costs as a broadband transducer is not required for simultaneous multiple transducer positioning. Then, a steepest descent optimization algorithm for precisely determining the 3D position of a transmitter was introduced. The unique features of the proposed steepest descent optimization algorithm over the traditional lateration algorithms are: it does not suffer from DOP errors; and is able to ignore the errors in the distance measurements of the receivers corresponding to one complete cycle of the transmitted signal.

The experimental results showed that, the proposed system is able to measure the 3D locations of multiple transducers with sub-millimeter accuracy which is significantly better than that of the alternative traditional approach.

Moreover, the proposed system can also be used in larger scale indoor positioning applications where location information needs to be stored centrally (e.g., in office environment and research labs) using an active mobile architecture and for those applications where user privacy is an issue (e.g., in museums, supermarkets, or government buildings) using a passive mobile architecture.

REFERENCES

[1] A. J. Weiss and E. Weinstein, "Fundamental limitations in passive time delay estimation—Part I: Narrow–band systems," *IEEE Trans. Acoust., Speech Signal Process.*, vol. 31, no. 2, pp. 472–486, 1983.

[2] S. Widodo *et al.*, "Moving object localization using sound-based positioning system with doppler shift compensation," *Robotics*, vol. 2, no. 2, pp. 36–53, 2013.

[3] A. Yazici, U. Yayan, and H. Yücel, "An ultrasonic based indoor positioning system," in *Proc. Int. Symp. Innov. Intell. Syst. Appl.*, 2011, pp. 585–589.

[4] T. Hori and Y. Nishida, "Improvement of position estimation of the ultrasonic 3D tag system," in *Proc. 17th IEEE Int. Symp. Robot Human Interact. Commun.*, Aug. 2008, pp. 436–441.

[5] A. Sanchez, A. de Castro, S. Elvira, G. Glez-de-Rivera, and J. Garrido, "Autonomous indoor ultrasonic positioning system based on a low-cost conditioning circuit," *Measurement*, vol. 45, no. 3, pp. 276–283, 2012.

[6] F. Tatar, J. R. Mollinger, J. Bastemeijer, and A. Bossche, "Time of flight technique used for measuring position and orientation of laparoscopic surgery tools," in *Proc. IEEE Sensors*, vol. 3, Oct. 2004, pp. 1480–1483.

[7] Y. Zejie, Y. Yanming, W. Qihang, and L. Wenlian, "A new system for three-dimensional kinematic trajectory acquisition and analysis—I. The application of an ultrasonic technique to human gait analysis," *Med. Eng. Phys.*, vol. 18, no. 5, pp. 420–426, 1996.

[8] Y. Zejie, Y. Yanming, L. Wenlian, and W. Qihang, "A new system for three–dimensional kinematic trajectory acquisition and analysis—II. Digital orthogonal integration phase–detection technique," *Med. Eng. Phys.*, vol. 18, no. 5, pp. 427–432, 1996.

[9] R. B. Huitema, A. L. Hof, and K. Postema, "Ultrasonic motion analysis system—Measurement of temporal and spatial gait parameters," *J. Biomech.*, vol. 35, no. 6, pp. 837–842, 2002.

[10] L. Vogt, M. Portscher, K. Brettmann, K. Pfeifer, and W. Banzer, "Cross-validation of marker configurations to measure pelvic kinematics in gait," *Gait Posture*, vol. 18, no. 3, pp. 178–184, 2003.

[11] R. M. Kiss, L. Kocsis, and Z. Knoll, "Joint kinematics and spatial–temporal parameters of gait measured by an ultrasound-based system," *Med. Eng. Phys.*, vol. 26, no. 7, pp. 611–620, 2004.

[12] A. Putzhammer, B. Heindl, K. Broll, L. Pfeiff, M. Perfahl, and G. Hajak, "Spatial and temporal parameters of gait disturbances in schizophrenic patients," *Schizophrenia Res.*, vol. 69, nos. 2–3, pp. 159–166, 2004.

[13] A. Putzhammer, M. Perfahl, L. Pfeiff, and G. Hajak, "Gait disturbances in patients with schizophrenia and adaptation to treadmill walking," *Psychiatry Clin. Neurosci.*, vol. 59, no. 3, pp. 303–310, 2005.

[14] G. Ogris, T. Stiefmeier, H. Junker, P. Lukowicz, and G. Troster, "Using ultrasonic hand tracking to augment motion analysis based recognition of manipulative gestures," in *Proc. 9th IEEE Int. Symp. Wearable Comput.*, Oct. 2005, pp. 152–159.

[15] T. Stiefmeier, G. Ogris, H. Junker, P. Lukowicz, and G. Troster, "Combining motion sensors and ultrasonic hands tracking for continuous activity recognition in a maintenance scenario," in *Proc. 10th IEEE Int. Symp. Wearable Comput.*, 2006, pp. 97–104.

[16] Y. Wahab, "Design and implementation of MEMS biomechanical sensors for real-life measurements of gait parameters," Ph.D. dissertation, School Eng. Sci., Victoria Univ., Melbourne VIC, Australia, 2009.

[17] N. Hemmati and P. Rangraz, "Notice of violation of IEEE publication principles design of ultrasonic motion analysis system for estimating segment's stabilization during dynamic condition," in *Proc. IEEE EUROCON*, May 2009, pp. 134–137.

[18] T. Sato, S. Nakamura, K. Terabayashi, M. Sugimoto, and H. Hashizume, "Design and implementation of a robust and real-time ultrasonic motion-capture system," in *Proc. Int. Conf. Indoor Positioning Indoor Navigat.*, Sep. 2011, pp. 1–6.

[19] Y. Wahab and N. A. Bakar, "Gait analysis measurement for sport application based on ultrasonic system," in *Proc. ISCE*, Jun. 2011, pp. 20–24.

[20] J. Roggendorf, S. Chen, S. Baudrexel, S. van de Loo, C. Seifried, and R. Hilker, "Arm swing asymmetry in Parkinson's disease measured with ultrasound based motion analysis during treadmill gait," *Gait Posture*, vol. 35, no. 1, pp. 116–120, 2012.

[21] M. Domagalska, A. Szopa, M. Syczewska, S. Pietraszek, Z. Kidoń, and G. Onik, "The relationship between clinical measurements and gait analysis data in children with cerebral palsy," *Gait Posture*, vol. 38, no. 4, pp. 1038–1043, 2013.

[22] C. A. Macleod, B. A. Conway, D. B. Allan, and S. S. Galen, "Development and validation of a low-cost, portable and wireless gait assessment tool," *Med. Eng. Phys.*, vol. 36, no. 4, pp. 541–546, 2014.

[23] Y. Qi, C. BoonSoh, E. Gunawan, K.-S. Low, and A. Maskooki, "A novel approach to joint flexion/extension angles measurement based on wearable UWB radios," *IEEE J. Biomed. Health Informat.*, vol. 18, no. 1, pp. 300–308, Jan. 2014.

[24] Y. Qi, C. B. Soh, E. Gunawan, and K.-S. Low, "Ambulatory measurement of three-dimensional foot displacement during treadmill walking using wearable wireless ultrasonic sensor network," *IEEE J. Biomed. Health Inform.*, vol. 19, no. 2, pp. 446–452, Mar. 2014.

[25] Y. Wahab, M. Mazalan, N. A. Bakar, A. F. Anuar, M. Z. Zainol, and F. Hamzah, "Low power shoe integrated intelligent wireless gait measurement system," *J. Phys., Conf. Ser.*, vol. 495, no. 1, p. 012044, 2014.

[26] R. Queirós, F. C. Alegria, P. S. Girao, and A. C. Serra, "Cross-correlation and sine-fitting techniques for high-resolution ultrasonic ranging," *IEEE Trans. Instrum. Meas.*, vol. 59, no. 12, pp. 3227–3236, Dec. 2010.

[27] M. Addlesee *et al.*, "Implementing a sentient computing system," *Computer*, vol. 34, no. 8, pp. 50–56, Aug. 2001.

[28] M. Hazas and A. Ward, "A high performance privacy-oriented location system," in *Proc. 1st IEEE Int. Conf. Pervasive Comput. Commun.*, Mar. 2003, pp. 216–223.

[29] M. Hazas and A. Hopper, "Broadband ultrasonic location systems for improved indoor positioning," *IEEE Trans. Mobile Comput.*, vol. 5, no. 5, pp. 536–547, May 2006.

[30] J. R. Gonzalez and C. J. Bleakley, "High-precision robust broadband ultrasonic location and orientation estimation," *IEEE J. Sel. Topics Signal Process.*, vol. 3, no. 5, pp. 832–844, Oct. 2009.

[31] M. M. Saad, C. J. Bleakley, T. Ballal, and S. Dobson, "High-accuracy reference-free ultrasonic location estimation," *IEEE Trans. Instrum. Meas.*, vol. 61, no. 6, pp. 1561–1570, Jun. 2012.

[32] C. Sertatıl, M. A. Altınkaya, and K. Raoof, "A novel acoustic indoor localization system employing CDMA," *Digit. Signal Process.*, vol. 22, no. 3, pp. 506–517, 2012.

[33] P. K. Misra, "Acoustical localization techniques in embedded wireless sensor networked devices," Ph.D. dissertation, Dept. Comput. Sci. Eng., Univ. New South Wales, Sydney, NSW, Australia, 2012.

[34] W. E. Moritz, P. L. Shreve, and L. E. Mace, "Analysis of an ultrasonic spatial locating system," *IEEE Trans. Instrum. Meas.*, vol. 25, no. 1, pp. 43–50, Mar. 1976.

[35] L. Kleeman, "Ultrasonic autonomous robot localisation system," in *Proc. IROS*, Sep. 1989, pp. 4–6.

[36] L. Kleeman, "Iterative algorithm for three dimensional autonomous robot localisation," in *Proc. 3rd Nat. Conf. Robot.*, Jun. 1990, pp. 210–219.

[37] L. Kleeman, "A three dimensional localiser for autonomous robot vehicles," *Robotica*, vol. 13, no. 1, pp. 87–94, Jan. 1995.

[38] J. Hightower and G. Borriello, "Location systems for ubiquitous computing," *Computer*, vol. 34, no. 8, pp. 57–66, 2001.

[39] A. Harter, A. Hopper, P. Steggles, A. Ward, and P. Webster, "The anatomy of a context-aware application," *J. Wireless Netw.*, vol. 8, nos. 2–3, pp. 187–197, Mar. 2002.

[40] N. B. Priyantha, A. Chakraborty, and H. Balakrishnan, "The cricket location-support system," in *Proc. 6th Annu. Int. Conf. Mobile Comput. Netw.*, 2000, pp. 32–43.

[41] C. Randell and H. Muller, "Low cost indoor positioning system," in *Proc. Int. Symp. Ubiquitous Comput.*, 2001, pp. 42–48.

[42] A. Smith, H. Balakrishnan, M. Goraczko, and N. B. Priyantha, "Tracking moving devices with the cricket location system," in *Proc. 2nd Int. Conf. Mobile Syst., Appl. Services*, Jun. 2004, pp. 190–202.

[43] M. R. McCarthy, "The BUZZ: Narrowband ultrasonic positioning for wearable computers," Ph.D. dissertation, Dept. Comput. Sci., Univ. Bristol, Bristol, U.K., 2007.

[44] X. Li, K. Pahlavan, M. Latva-Aho, and M. Ylianttila, "Comparison of indoor geolocation methods in DSSS and OFDM wireless LAN systems," in *Proc. 52nd IEEE Veh. Technol. Conf.*, vol. 6. Sep. 2000, pp. 3015–3020.

[45] J. Li, "Characterization of WLAN location fingerprinting systems," M.S. thesis, Dept. Inst. Comput. Syst. Archit., School Inform., Univ. Edinburgh, Edinburgh, U.K., 2012.

[46] T. Kitasuka, T. Nakanishi, and A. Fukuda, "Design of WiPS: WLAN—Based indoor positioning system," *Korea Multimedia Soc.*, vol. 7, no. 4, pp. 15–29, 2003.

[47] J. D. Gupta, H. Suzuki, and K. Ziri-Castro, "Effect of pedestrian movement on MIMO-OFDM channel capacity in an indoor environment," *IEEE Antennas Wireless Propag. Lett.*, vol. 8, pp. 682–685, Jun. 2009.

[48] T. J. S. Khanzada, "Wireless communication techniques for indoor positioning and tracking applications," Ph.D. dissertation, Faculty Elect. Eng. Inf. Technol., Magdeburg Univ., Magdeburg, Germany, 2010.

[49] B. Pricope and H. Haas, "Experimental validation of a new pedestrian speed estimator for OFDM systems in indoor environments," in *Proc. IEEE Global Telecommun. Conf.*, Dec. 2011, pp. 1–5.

[50] J. Xiao, K. Wu, Y. Yi, and L. M. Ni, "FIFS: Fine-grained indoor fingerprinting system," in *Proc. 21st Int. Conf. Comput. Commun. Netw.*, Jul. 2012, pp. 1–7.

[51] K. Wu, J. Xiao, Y. Yi, D. Chen, X. Luo, and L. M. Ni, "CSI-based Indoor Localization," *IEEE Trans. Parallel Distrib. Syst.*, vol. 24, no. 7, pp. 1300–1309, Jul. 2013.

[52] B. Pricope and H. Haas, "Positioning using terrestrial wireless systems," Ph.D. dissertation, Dept. Elect. Eng., Jacobs Univ. Bremen, Bremen, Germany, 2013.

[53] M. Shafiee, "WiFi-based fine timing assistance for GPS acquisition," Ph.D. dissertation, Dept. Geomatics Eng. Univ. Calgary, Calgary, AB, Canada, 2003.

[54] J. D. Ashdown, G. J. Saulnier, T. J. Lawry, K. R. Wilt, and H. A. Scarton, "High-rate ultrasonic communication through metallic barriers using MIMO-OFDM techniques," in *Proc. Military Commun. Conf.*, Oct./Nov. 2012, pp. 1–6.

[55] K. Wanuga, M. Bielinski, R. Primerano, M. Kam, and K. R. Dandekar, "High-data-rate ultrasonic through-metal communication," *IEEE Trans. Ultrason., Ferroelectr., Freq. Control*, vol. 59, no. 9, pp. 2051–2053, Sep. 2012.

[56] T. J. Lawry, K. R. Wilt, J. D. Ashdown, H. A. Scarton, and G. J. Saulnier, "A high-performance ultrasonic system for the simultaneous transmission of data and power through solid metal barriers," *IEEE Trans. Ultrason., Ferroelectr., Freq. Control*, vol. 60, no. 1, pp. 194–203, Jan. 2013.
[57] W. M. D. Wright, O. M. Doyle, and C. T. Foley, "P2I-9 multi-channel data transfer using air-coupled capacitive ultrasonic transducers," in *Proc. IEEE Ultrason. Symp.*, Oct. 2006, pp. 1805–1808.
[58] W. N. Venables and B. D. Ripley, "Robust statistics," in *Modern Applied Statistics With S-PLUS*. New York, NY, USA: Springer, 1999, pp. 247–266.
[59] S. Boyd and L. Vandenberghe, *Convex Optimization*. Cambridge, U.K.: Cambridge Univ. Press, 2004.

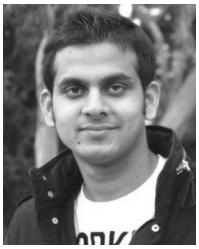

Md. Omar Khyam was born in Chittagong, Bangladesh, in 1988. He received the B.Sc. degree in electronics and telecommunication engineering from the Rajshahi University of Engineering and Technology, Rajshahi, Bangladesh, in 2010, and the Ph.D. degree from the University of New South Wales, in 2015. He is currently working as a Postdoctoral Research Fellow at National University of Singapore. His research interests include ultrasonic signal processing for biomedical and industrial applications.

Md. Jahangir Alam received the B.Sc. degree in computer science and engineering from the Rajshahi University of Engineering and Technology, Rajshahi, Bangladesh, in 2006, and the Ph.D. degree from the University of New South Wales, Australia, in 2013.

He is currently a Software Developer. His research interests include image coding, digital signal processing, and underwater acoustics.

Andrew J. Lambert received the B.Sc. (Hons.) degree in physics from the University of Otago, New Zealand, in 1984, and the Ph.D. degree in electrical engineering from the University of New South Wales at Canberra, Australia, in 1997.

He has been a Lecturing Staff member with the University of New South Wales at Canberra since 1988. His research interests include optical and digital image and signal processing, high speed processing hardware, electro-optics and adaptive optics for imaging through turbulence applications in astronomy, surveillance, and ophthalmology as well as for holographic video display.

Matthew A. Garratt received the Ph.D. degree in robotics from Australian National University (ANU) in 2007. He worked for over a decade as an Aeronautical Engineer with the Royal Australian Navy, before working for two years in the field of computer-aided engineering tools. In 1999, he joined ANU, where he helped build and test an autonomous helicopter using biologically inspired vision for a DARPA funded project. Since 2001, he has been with the School of Engineering and Information Technology, University of New South Wales at Canberra, Australia, as a Lecturer. His main research areas are sensing and control for autonomous systems.

Mark R. Pickering (S'92–M'95) was born in Biloela, Australia, in 1966. He received the B.Eng. degree from the Capricornia Institute of Advanced Education, Rockhampton, Australia, in 1988, and the M.Eng. and Ph.D. degrees from the University of New South Wales at Canberra, Australia, in 1991 and 1995, respectively, all in electrical engineering.

He was a Lecturer from 1996 to 1999 and a Senior Lecturer from 2000 to 2009 with the School of Electrical Engineering and Information Technology, University of New South Wales, where he is an Associate Professor. His research interests include video and audio coding, medical imaging, data compression, information security, data networks, and error-resilient data transmission.